CHARACTERIZATION OF AN EXPLOSION SOURCE IN A COMPLEX MEDIUM BY MODELING AND WAVELET DOMAIN INVERSION

M. Nafi Toksöz, Xu Li, Mary Krasovec, and Shihong Chi

Massachusetts Institute of Technology

Sponsored by Air Force Research Laboratory

Contract No. F19628-03-C-0126

ABSTRACT

Explosions are often conducted in complexes with chambers, tunnels, and shafts used for access and instrumentation. These structures can act as strong scatterers of seismic waves and complicate the radiation patterns from explosions. The objectives of this project are (1) to study the effects of these near-source scatterers on seismic waves radiated from explosions, and (2) to use a wavelet domain based moment-tensor inversion scheme to determine “explosive” and “multicouple” components of the source.

During the first phase of the project, emphasis has been on forward modeling. A three-dimensional (3-D) variable grid finite-difference code was used to model the effects of cylindrical cavities located near an explosion source. The presence of a cylinder results in strong scattering into P and S waves, and the reverberation of energy in the cylinder. Waves going around the cylinder and those reverberating inside continue to radiate long after the initial explosion. The observed wave trains are longer than those of the explosion alone. A cylinder near an explosive source scatters energy into P, SV, and SH waves. The P and S waves are separated by calculating the divergence and curl of the displacement fields. The relative significance of factors contributing to scattering (e.g., size, proximity to explosion, orientation, etc.) is investigated. Synthetic seismograms are used to test the performance of moment-tensor inversion and its ability to separate the volumetric and shear components of the source. With good azimuthal coverage, the moment-tensor shows significant shear components in the presence of a scatterer.

OBJECTIVE

An explosive source in a laterally homogeneous layered half-space generates P, SV, and Rayleigh waves, but not SH or Love waves. However, seismograms from a large number of explosions show nonisotropic radiation patterns for P and Rayleigh waves, and prominent SH and Love waves. The near-source contribution to nonisotropic radiation of P, Rayleigh and SH waves generated by an explosion can be attributed to three mechanisms. First is the tectonic strain energy released by the explosion, resulting in a composite source consisting of an explosion and a double couple (e.g., Archambeau and Sammis, 1970; Toksoz et al., 1965; Toksoz and Kehrer, 1972; Wallace et al., 1983, 1985; Priestley et al., 1990; Schlittenhardt, 1991; Stump et al., 1994; Patton and Taylor, 1995). The second factor that contributes to the nonisotropic seismic radiation pattern from explosive sources is the shape of the explosion cavity and the location of the explosive source in that cavity (Rial and Moran, 1986; Stevens et al., 1991; Zhao and Harkrider, 1992; Ben-Menahem and Mikhailov, 1995; Gibson et al., 1996; Ben-Menahem, 1997; Imhof and Toksöz, 2002). The third mechanism contributing to complex seismic radiation from an explosion is the near-source scattering (Gupta et al., 1990; Johnson, 1997; Ben-Menahem, 1997; Imhof and Toksöz, 2000, 2002). This mechanism could be significant when strong scatterers are present near the source.

The objective of this research is to study the role of scattering from near-source structures such as tunnels, shafts, adits, and surface topography in the generation of complicated radiation patterns and SH waves from explosions. In addition, the study will test the performance of moment-tensor inversion to separate the isotropic (i.e., explosion) and multicouple components of the source as an aid to seismic discrimination.

RESEARCH ACCOMPLISHED

A three-dimensional (3-D) finite-difference (FDTD) program was developed to model wave propagation and scattering in heterogeneous media. The program utilizes a variable grid implemented through a grid-stretching technique. The code is parallelized to be run on a computer cluster. Initial calculations were directed to 3-D forward modeling with an explosive source and a finite-length tunnel in a homogeneous medium. The calculations show strong P to P and P to S scattering and a complicated radiation pattern. A simple moment-tensor inversion using the calculated seismograms shows that there is a double couple component, but the isotropic component is still dominant over the double couple. The radiation pattern at high frequencies (40 Hz) is too complicated to be represented by a first-order moment-tensor.

Forward Modeling by the Finite Difference Approach

The time domain finite-difference method has been one of the most widely used tools to simulate wave propagation in 2-D and 3-D elastic media with spatial variations of elastic properties. Computational efficiency can be achieved by sampling the physical space adaptively with a variable grid. However, the variable grid can introduce wave distortion or numerical reflections due to phase change at the interface of two grids of different sizes (Browning et al., 1973). Numerical reflections can be eliminated by taking extra averages of solutions at the grid interface. However, wave distortion cannot always be avoided. Introducing a change in grid spacing may also adversely affect the formal truncation error and the stability of the system (Crowder and Dalton, 1971). In our finite difference algorithm, we apply a coordinate transformation, or stretching, to achieve effective variable grids in the physical domain and uniform grids in the transformed domain (Huang, 2003). Because the computation is carried out on a uniform grid, the formal truncation error and the stability properties of the finite-difference computation are preserved.

Strong scattering from a near-source tunnel is simulated with the FDTD algorithm described above. Figure 1 shows the 3-D geometry of the simulation model including a cylindrical tunnel. Simulations are also conducted with the tunnel absent. The infinite formation is modeled by a finite volume of 3000 m by 3000 m by 1100 m in the x, y, and z directions. Absorbing boundaries are placed at all six sides of the model to eliminate wave reflection. An explosion source with a center frequency of 40 Hz is excited in the center of the model. The length and radius of the cylindrical tunnel are 50 m and 15 m, respectively. The axis of the tunnel is parallel to the y axis of the Cartesian coordinate. The distance between the source and the tunnel is 30 m. The formation is a perfect Poisson medium, with compressional and shear wave velocities and density of 4000 m/s, 2300 m/s, and 2500 kg/m^3, respectively. Inside the tunnel, we assume a sound velocity of 340 m/s and a compressed air density of 200 kg/m^3. The grid size increases from 1 m near the source and cylinder tunnel to 10 m away from the source region. Examples of calculated seismograms are shown in Figure 2. The receiver plane is in the xy plane and 200 m above the source. The seismograms are along a line parallel to the x axis. Computations are made for an explosion alone (without a tunnel) and an explosion with a tunnel present.

The top row of Figure 2 shows the x and z components of the motion (velocity fields) when the tunnel is absent. As expected, only P waves are generated. When the tunnel is present near the explosion source, strong scattering occurs. The seismograms in the middle row of Figure 2 show that the strong shear waves are scattered from the tunnel. To demonstrate the effect of scattering, we subtract the explosion only seismograms from those with the explosion plus the tunnel. The bottom row of Figure 2 shows these strong scattered waves. These are both P and S scattering, and scattered S waves are larger than P waves. SH waves are also observed, but their amplitudes are much smaller than the x and z components.

The divergence and curl of the wavefield separate the compressional and shear components of the wavefield, respectively. Figure 3 shows snapshots of the divergence and curl of the velocity field at 60 ms on the xz, yz and xy planes passing through the origin of the coordinate system. One can clearly see the complex pattern of the scattering. The curl is zero inside the tunnel. The snapshots of the xz plane and xy plane reveal the vertical and horizontal cross section of the tunnel. The snapshot along the yz plane, parallel to the tunnel, shows the complexity introduced by the finite length of the tunnel.

Understanding the patterns of scattered waves will help us choose appropriate models for inversion of the source mechanism. In the xz plane, the shear wave energy is divided into four quadrants, and the shear waves are in-phase in the diagonal quadrants. Shear waves in the half-space above and below the xy plane are 180^o out of phase. The disturbance to the P wavefield, caused by scattering, can also be seen in the divergence field, but the scattering patterns are not as clear as those of the shear waves.

The presence of several tunnels creates very complicated scattered waves. Figure 4 shows one example of such a model, where there are six intersecting tunnels 30 meters below the surface. Two components of the seismic motion are shown.

Moment Tensor Inversion

We used synthetic seismograms with an explosion and a strong scatterer near the source to test the performance of the first-order moment-tensor inversion. A simple frequency-domain inversion method was used (Stump and Johnson, 1997; Li and Chen, 1996).

We used three sets of seismograms: explosion alone, explosion plus a tunnel, and a scattered field only. The scattered signals were obtained by subtracting the pure explosion seismograms from the explosion plus tunnel seismograms, as shown in the bottom row of Figure 2.

Figure 5 shows the results of the first-order moment-tensor inversion. For an explosion without a tunnel, only the diagonal components of the moment-tensor (m11, m22, and m33) are nonzero. For an explosive source and a nearby tunnel, the nondiagonal components appear, but the explosion term still dominates. Even with purely scattered waves, the diagonal components of the moment-tensor are larger than the off-diagonal components. This suggests the need of a more realistic representation of the source with the inclusion of a higher-order tensor (Knopoff and Randall, 1970; Aki and Richards, 1980).

CONCLUSIONS AND RECOMMENDATIONS

Time domain finite-difference modeling of seismic waves from an explosion source in the presence of a nearby tunnel shows a complex scattering pattern. The tunnel acts as a scatterer and a secondary source radiating both P and S waves.

The results shown in this paper are for a high frequency source (40 Hz center frequency) in a relatively high-velocity medium (Vp = 4000 m/s; Vs = 2300 m/s). A high-frequency source was chosen to test the stability of the variable grid code. In addition, the high-frequency source provided high-resolution examples of the scattering phenomena. New models are being computed in the 1–10 Hz frequency range to generate representative seismograms.

Seismic waves generated by an explosion plus a strong scatter cannot be represented adequately by a single first-order moment tensor. The performance of the first-order moment-tensor representation at low frequencies needs to be tested.

REFERENCES

Aki, K., and P.G. Richards (1980), *Quantitative Seismology*, *Vol. 1,* Freeman and Company, New York.

Archambeau, C.B., and C. Sammis (1970) Seismic Radiation from Explosions in Prestressed Media and the Measurement of Tectonic Stress in the Earth, *Rev. Geophys*., 8, 473-499.

Ben-Menahem, A. (1997), Seismic Source Functions for Explosions in a Non-Spherical Cavity Embedded in a Scattering Environment: Application to the Regional Discrimination of Nuclear Explosion and Earthquakes. *Geophys. J. Int*., 128, 97-124.

Ben-Menahem, A., and O. Mikhailov (1995), Multiple Radiation of Seismic Waves from Explosions in Non-Spherical Cavities and its Application to Signal Identification, *J. Acoust. Soc. Am*., 97, 2675-2698.

Browning, G., H.O. Kreiss, and J. Oliger (1973), Mesh Refinement, *Mathematics of Computation,* 27, 29-39.

Crowder, H.J., and C. Dalton, C. (1971), Errors in the use of Nonuniform Mesh Systems, *J. Computational Physics,* 7, 32-45.

Gibson, R. L., M. N. Toksöz, and W. Dong (1996), Seismic Radiation from Explosively Loaded Cavities in Isotropic and Transversely Isotropic Media, *Bull. Seism. Soc. Am.,* 86, 1910-1924.

Gupta, I. N., C. S. Lynnes, T. W. McElfresh, and R. A. Wagner (1990), F-K Analysis of NORESS Array and Single Station Data to Identify Sources of Near-Receiver and Near-Source Scattering, *Bull. Seism. Soc. Am.*, 80, 2227-2241.

Huang, X (2003), Effects of Tool Positions on Borehole Acoustic Measurements: A Stretched Grid Finite Difference Approach, Ph.D. Thesis, Massachusetts Institute of Technology.

Imhof, M.G. and M.N. Toksöz (2000), Scattering from Tunnels Near Sources and their Effects on Seismic Signatures of Explosions. *Bull. Seism. Soc. Am*., 90, 229-242.

Imhof , M. G. and M. N. Toksöz (2002), The Effects of Synchronized Multiple-Cavity Sources on Seismic Radiation. *Bull. Seism. Soc. Am*., 92, 2381-2390.

Johnson, L. R. (1997), Generation of S Waves by Explosion, in *Proceedings of 19th Annual Seismic Research Symposium on Monitoring a Comprehensive Test Bay Treaty (CTBT),* M. J. Shore, R. S. Jih, A. Dainty, and Erwin (eds.), Defense Special Weapons Agency, 625-631.

Knopoff, L., and M. Randall, M. (1970), The Compensated Linear-Vector Dipole: A Possible Mechanism for Deep Earthquakes, *J. Geophys. Res.,* 75, 4957-4963.

Li, X. and Y.T. Chen (1996), Inversion of Long-Period Body-Wave Data for the Source Process of the Gonghe, Qinghai, China Earthquake, *Acta Seismologica Sinica*, 9, 361~369.

Patton, H.J. and S.R. Taylor (1995), Analysis of Lg Spectral Ratios from NTS Explosions: Implications for the Source Mechanisms of Spall and the Generation of Lg Waves, *Bull. Seism. Soc. Am*., 85, 220-236.

Priestley, K.F., W.R. Walter, V. Martynov, and M.V. Rozhkov (1990). Regional Seismic Recordings of the Soviet Nuclear Explosion of the Joint Verification Experiment, *Geophys. Res. Lett*., *17*, 179-182.

Rial, J.A., and B. Moran (1986). Radiation Patterns for Explosive-Loaded Axisymmetric Cavities in an Elastic Medium: Analytic Approximations and Numeric Results. *Geophys. J. R. Astr. Soc*., *86*, 855-862.

Schlittenhardt, J. (1991). The Effects of Spall on Teleseismic P-Waves: an Investigation with Theoretical Seismograms, in *Explosion Source phenomenology*, S. Taylor, H. Patton, and P. Richards (eds.), American Geophysical Union, Washington, D.C., 141-150.

Stevens, J.L, J.R. Murphy, and N. Rimer (1991). Seismic Source Characteristics of Cavity Decoupled Explosions in Salt and Tuff, *Bull. Seism. Soc. Am*., *81*, 4, 1272-1291.

Stump, B.W., and Johnson, L.R. (1977). The Determination of Source Properties by the Linear Inversion of Seismograms, *Bull. Seism. Soc. Am.*, *67*, 1489–1502.

Stump, B.W., R.E. Reinke, K.H. Olson, and L.R. Johnson (1994). Isotropic and Deviatoric Characterization of the Coalora Nuclear Explosion in Yucca Flats, *Geophys. J. Int*., *116*, 538-552.

Toksöz, M.N., D.G. Harkrider, and A. Ben-Menahem (1965). Determination of Source Parameters by Amplitude Equalization of Seismic Surface Waves: Part 2, Release of Tectonic Strain by Underground Nuclear Explosions and Mechanisms of Earthquakes*, J. Geophys. Res*., *70*, 907-922.

Toksöz, M.N., and H.H. Kehrer (1972). Tectonic Strain Release by Underground Nuclear Explosions and its Effect on Seismic Discrimination, *Geophys. J. R. Astr. Soc*., *31*, 141-161.

Wallace, T.C., D.V. Helmberger, and G.R. Engen (1983). Evidence of Tectonic Release from Underground Nuclear Explosions in Long-Period P-Waves, *Bull. Seism. Soc., Am*., *73*, 593-613.

Wallace, T.C., D.V. Helmberger, and G.R. Engen (1985). Evidence of Tectonic Release from Underground Nuclear Explosions in Long-Period S-Waves, *Bull. Seism. Soc. Am.*, *75*, 157-174.

Zhao, L. and D.G. Harkrider (1992). Wavefield from an Off-Center Explosion in an Embedded Solid Sphere, *Bull. Seism. Soc. Am., 82*, 1927-1955.

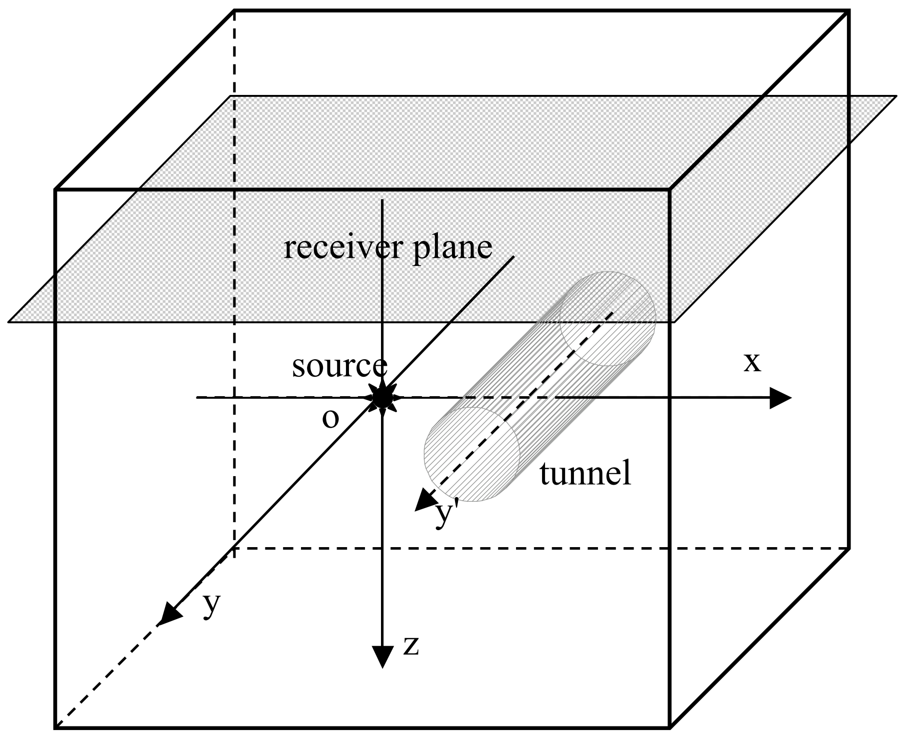

Figure 1. The geometry skeleton diagram of the model discussed in this paper. The explosion source is set in the middle of the model, coincident with the origin of the coordinates. A cylindrical tunnel is set 30 m away from the source, with radius of 15 m and length of 50 m. Its symmetric axis is parallel to the y axis. The receivers are set in the plane 200 m above the source. The distance between the neighbor receivers is 100 m. The medium parameters can refer to the context.

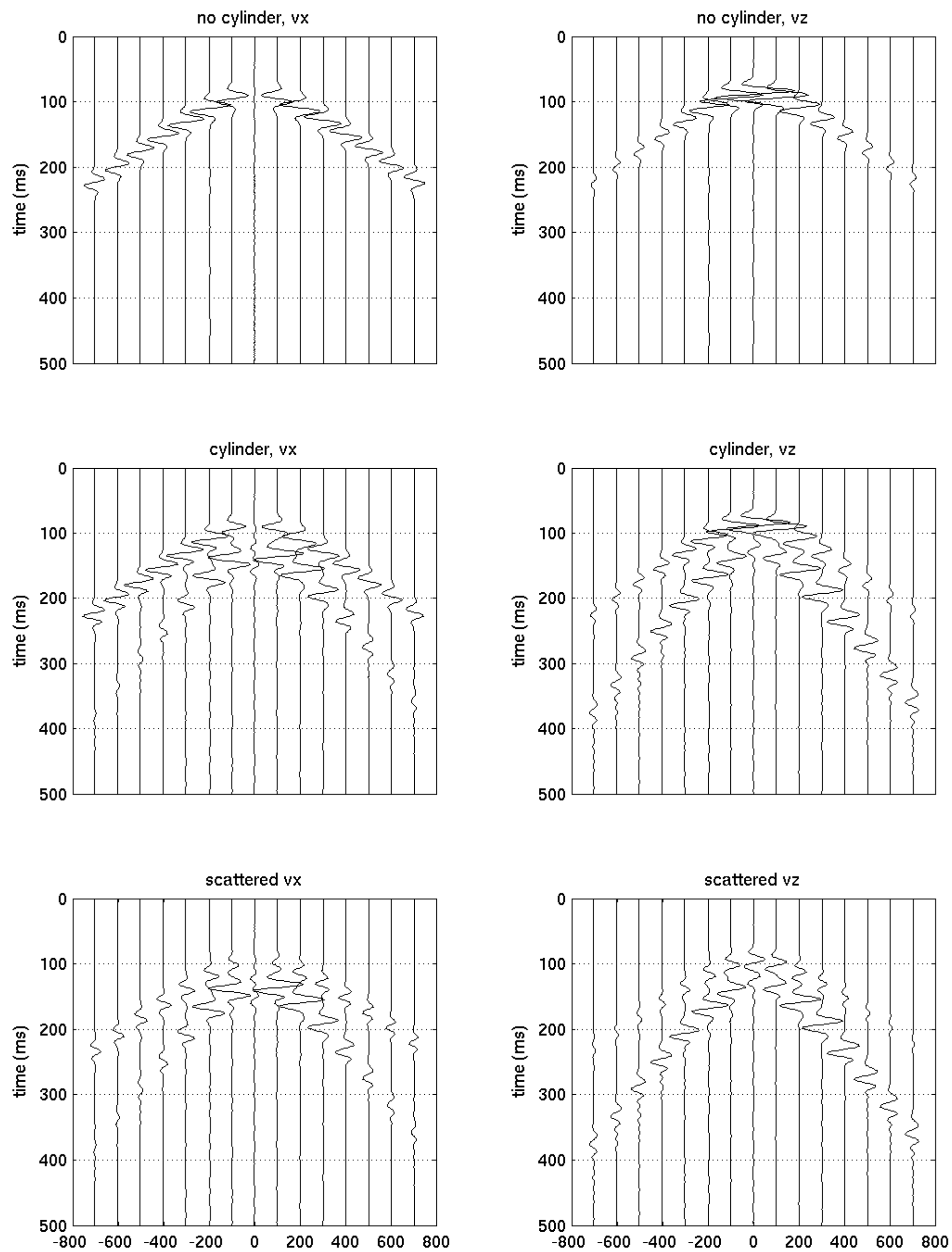

Figure 2. Comparison of the x and z components of the velocity fields at the receiver plane in the absence and the presence of the tunnel. Respective scattered velocity fields of the x and z components are also shown in the bottom row of this figure.

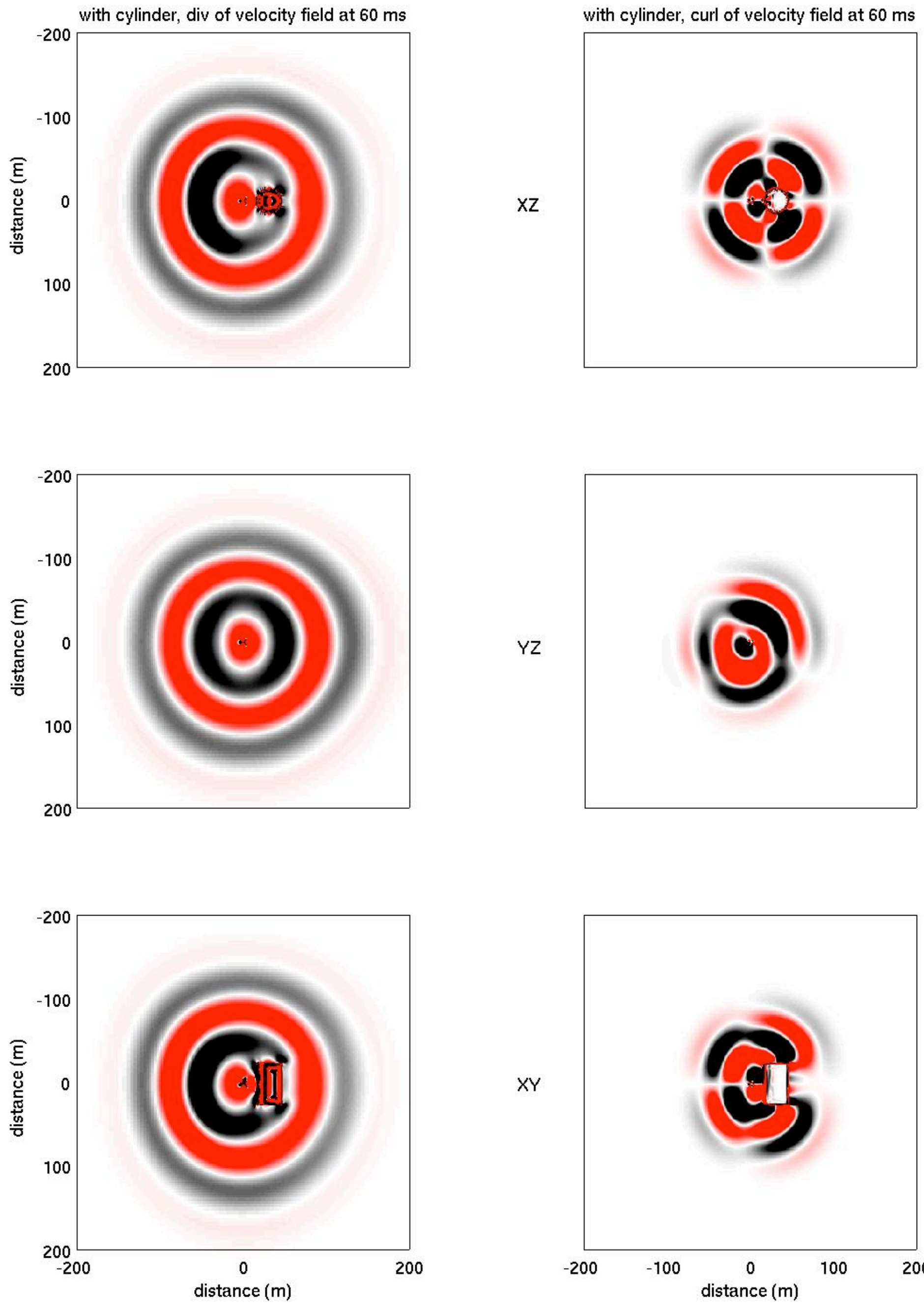

Figure 3. Snapshots of the divergence and curl of the velocity field from an explosion in the presence of a near-source tunnel. The snapshots were taken at 60 ms after the explosion.

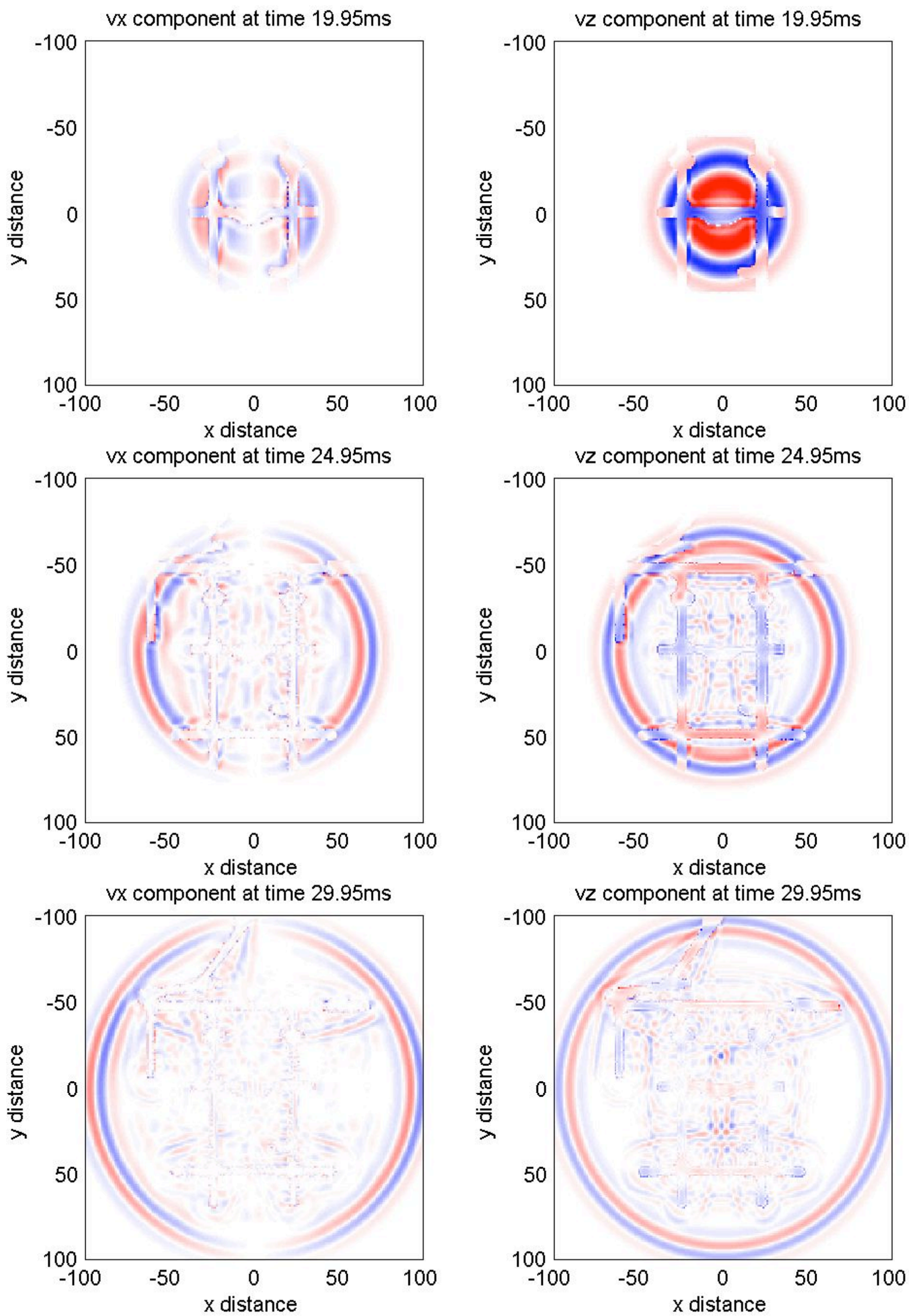

Figure 4. An example of the scattered wave propagating in a complex tunnel structure. There are six intersecting tunnels. Snapshots of Vx and Vz were taken above the model.

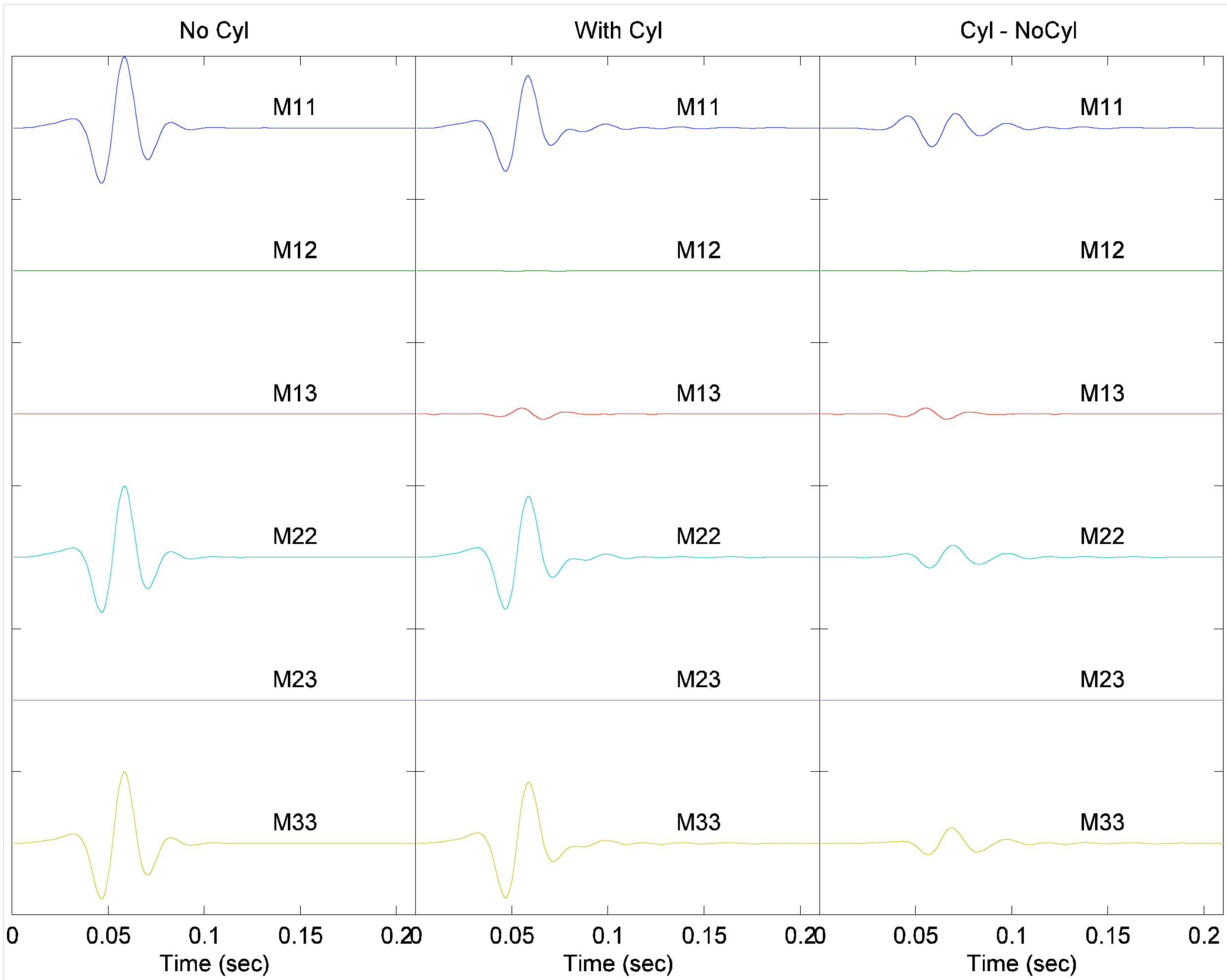

Figure 5. The results of moment-tensor inversion for an explosion alone (left), an explosion with a nearby cylindrical tunnel (middle), and pure scattered signals (right). Even for pure scattered signals, the isotropic component is still dominant. The large amplitude of M13, relative to other two deviatoric components M12 and M23, suggests that the radiation pattern could be related to the geometry property of the tunnel.